AADE-11-NTCE-66

Improved LWD Density Images in the Presence of Cyclic Borehole Noise

Junichi Sugiura and Jun Zhang, PathFinder®, A Schlumberger Company

Abstract

The use of logging-while-drilling (LWD) imaging tools has become commonplace. However, image noise and processing errors due to the inherent measurement physics can propagate errors and thus complicate interpretation of open-hole log data and images. For example, the standard density images tend to amplify image noise from small borehole irregularities, such as those from borehole spiral. When the cyclic noise amplitude from spiraling becomes large relative to the measurement of the primary interest, it largely affects measurement accuracy of bulk density, photoelectric, and neutron porosity.

Frequency-domain filtering using discrete Fourier transform has been used in the past to eliminate cyclic noise[1,2,3]. Although these techniques are relatively simple in concept, they are seldom used especially for two-dimensional applications due to implementation issues requiring interactive filter design. This paper shows a new way to remove cyclic noise from formation evaluation (FE) images by applying frequency-domain filtering. Stand-alone software has been developed to process the entire image logs from one well, without human supervision.

To quantitatively examine the validity of using these kinds of transformation-based filters, the algorithm is applied to field data as well as simulated data. The new algorithm has been proved to improve the image quality considerably without any artificial interruptions. The rugosity effect is significantly reduced, and the apparent resolution of bed boundary features increased. Comparative field examples illustrate the improvement in image feature extraction. This new method is critical, for example, for small fracture detection and for accurate dip analysis in irregular boreholes. This new method is not only effectively used for density images but also applicable to any other borehole images, such as resistivity and ultrasonic images.

Introduction

It is well known that poor hole quality causes degraded LWD and wireline log quality. Even though some practical guidelines on bit/BHA designs for better hole quality have been published in the past, borehole oscillation problems still occur and consequently, affect negatively on the interpretations of FE images.

LWD density images, for example, were originally introduced to improve the bulk density measurement accuracy in a certain azimuthal direction. However, now it has become a standard application for geosteering in which particular bed boundary information is critical and a bed dip angle calculation can enhance the accurate placement of the well. When borehole oscillation becomes severe, the oscillation noise often distorts and masks critical formation information such as small fractures and accurate dip analysis in FE images.

This paper presents a new way of removing cyclic borehole noise from FE images using two-dimensional discrete Fourier transform. Basic mathematical formulae regarding the new technique are provided, and its concept is demonstrated with simulated, noisy FE images.

Stand-alone software has been developed to examine the effectiveness of the new noise removal method. New features of the software algorithm that enhance the two-dimensional frequency-domain filtering are explained.

Some field examples show the improvement in the FE images when this new method is applied.

Frequency-Domain Filtering

This section explains the two-dimensional (2-D) discrete Fourier transform (DFT) and inverse DFT and how they are used to remove cyclic borehole noise from finite-extent FE images. To demonstrate the process, a simulated oscillation noise is created using finite-extent two-dimensional discrete-space sinusoids. A few types of the simulated noise are added to a clean FE image. Only pure 2-D sinusoids are used for demonstration purposes.

Simplified Notation for Complex Exponential

A finite-extent image $f(m, n)$ can be expressed as a matrix $\boldsymbol{f} = [f(m, n);\ 0 \le m \le M\text{-}1,\ 0 \le n \le N\text{-}1]$. Later in the section, discrete Fourier transform (DFT) will be applied to this image. To simplify the complex exponential notation used in DFT (also in inverse DFT), the below expression will be used in this paper:

$$W_K = e^{-i\frac{2\pi}{K}} = \exp\left[-i\frac{2\pi}{K}\right] \qquad (1)$$

as a simplified expression for the basic complex exponential, where $i = \sqrt{-1}$ is the pure imaginary number and K is the dimension along one of the image axes ($K = N$ or $K =$

M). Using the above expression, the various elementary frequency components at arbitrary spatial and frequency coordinates can be expressed as follows:

$$W_M^{um} W_N^{vn} = \cos\left[2\pi\left(\frac{u}{M}m + \frac{v}{N}n\right)\right] - i\sin\left[2\pi\left(\frac{u}{M}m + \frac{v}{N}n\right)\right] \qquad (2)$$

This process of space and frequency indexing by exponentiation greatly simplifies the manipulation of frequency components and the definition of the discrete Fourier transform.

Two-Dimensional Discrete Fourier Transform (DFT)

The two-dimensional discrete Fourier transform of the finite-extent ($M \times N$) image ***f*** is given by:

$$F(u,v) = \sum_{m=0}^{M-1}\sum_{n=0}^{N-1} f(m,n) W_M^{um} W_N^{vn} \qquad (3)$$

For integer frequencies $0 \le u \le M\text{-}1$, $0 \le v \le N\text{-}1$, hence, the DFT is also of finite extent $M \times N$, and can be expressed as a complex valued matrix $\boldsymbol{F} = [F(u, v);\ 0 \le u \le M\text{-}1,\ 0 \le v \le N\text{-}1]$.

Inverse Discrete Fourier Transform (IDFT)

The complex valued matrix ***F*** has a unique inverse discrete Fourier transform, or IDFT:

$$f(m,n) = \frac{1}{MN}\sum_{u=0}^{M-1}\sum_{v=0}^{N-1} F(u,v) W_M^{-um} W_N^{-vn} \qquad (4)$$

For $0 \le m \le M\text{-}1$, $0 \le n \le N\text{-}1$. **Equations 3** and **4** form a *DFT pair*. One interesting observation is that the DFT and IDFT are symmetrical; hence both forward and inverse transforms are defined as sums. In fact, they have the same form, except for the polarity of the exponents and a scaling factor. Both *f* and *F* can be represented as finite weighted sums of finite-extent complex exponentials with integer-indexed frequencies. It should be noticed that the frequency *(u, v)* are scaled so that their units are in cycles/image.

Two-Dimensional Discrete-Space Sinusoids

Two-dimensional frequency component, or sinusoidal function, is characterized not only by its location and its frequency of oscillation, but also by its direction of oscillation.

Two-dimensional discrete-space sinusoid has the following form:

$$\sin[2\pi(Um + Vn)] \qquad (5)$$

Equation 5 has two frequencies, *U* and *V* (unlike a one-dimensional sinusoid). These frequencies (with the units of cycles/pixel) represent the frequency of oscillation along the vertical (*m*) and horizontal (*n*) spatial image dimensions.

In practice, discrete images are confined to finite $M \times N$ sampling grid and it will be more convenient to utilize *finite-extent (M × N) two-dimensional discrete-space sinusoids*, which are defined only for integers:

$$0 \le m \le M-1,\ 0 \le n \le N-1 \qquad (6)$$

and undefined elsewhere. Two-dimensional sinusoid (5) defined on the finite grid (6) can be re-written as:

$$\sin\left[2\pi\left(\frac{u}{M}m + \frac{v}{N}n\right)\right] \qquad (7)$$

The following figures show several discrete-space sinusoids of dimensions 256 × 64 displayed as intensity images after linear mapping the gray scale of each to the range 0-255. In the figures, the image's vertical axis is equivalent to 128ft (256 pixels), while the pitch (wavelength) of the sinusoids is represented as 4ft/cycle and 8ft/cycle.

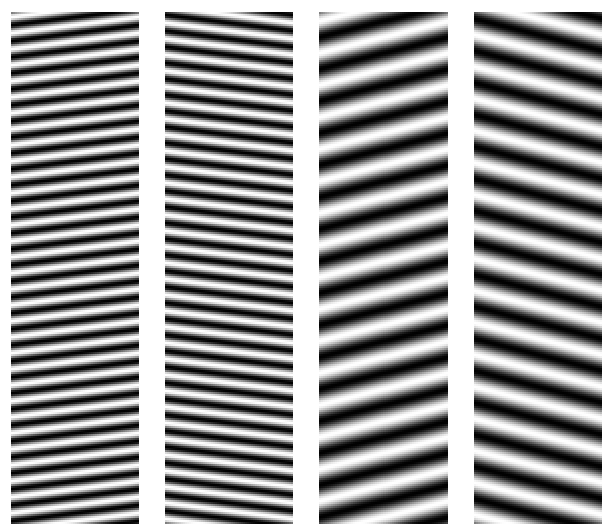

(1a) (1b) (1c) (1d)
u = 32 and v = 1 u = 16 and v = 1

Figure 1a, 1b, 1c and 1d: Two-dimensional discrete sinusoids

Figures 1a and **1b** have an oscillation pitch (wavelength) of 4ft/cycle, which is equivalent to 32 peaks per 128 ft (256 pixels) in a vertical direction. Their frequencies are u = 32 and v = 1, respectively. **Figures 1c** and **1d** have an oscillation pitch (wavelength) of 8ft/cycle, which is equivalent to 16 peaks per 128 ft (256 pixels). Their frequencies are u = 16 and v = 1, respectively.

As one can notice, the two-dimensional sinusoids look like formation-evaluation (FE) image noise caused by a spiral borehole. In fact, the Spiral Noise Removal algorithm discussed in this paper tries to identify the frequency of two-dimensional sinusoids and remove sinusoidal rugosity effects from noisy FE images.

Two-Dimensional Frequency-Domain Notch Filter

In the electronics industry, frequency-domain filtering using DFT has been utilized for decades. A typical application is to remove cyclic noise using notch (band-stop) filter centered at the frequency of the sinusoidal noise (for example rejecting 60Hz AC noise coming from a power line).

This notch filter concept can be applied to finite-extent two-dimensional images. Namely, we take the DFT of a given FE image, multiply the DFT coefficients with a frequency mask (notch filter mask) in the DFT domain, and take the IDFT of the product to bring the filtered image back to the space domain.

By masking (multiplying) the DFT ***F*** of an image ***f*** with a zero-one image frequency masks, one can produce, following an inverse DFT, a resulting image rejecting certain frequencies (e.g. unwanted spiral oscillation frequencies).

Figures 2a, 2b, 2c, and **2d** below show the DFTs of the sinusoidal images from **Figures 1a, 1b, 1c,** and **1d.**

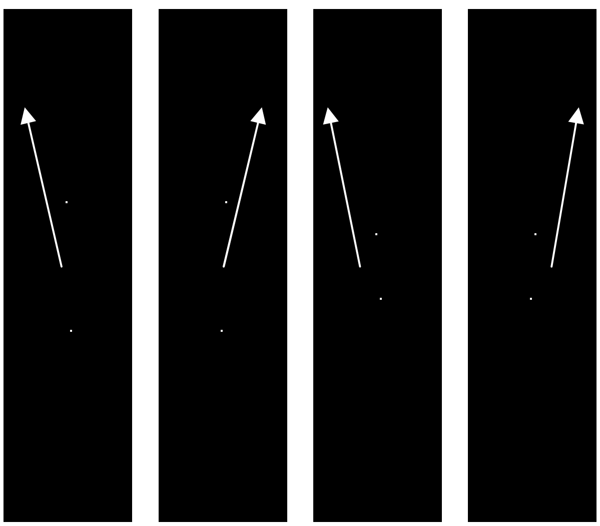

Figure 2a, 2b, 2c and 2d: The DFTs of the discrete sinusoids

Each of the original sinusoidal images in **Figures 1a, 1b, 1c,** and **1d** contains a strong directional component, which appears as a very strong peak point locating right or left side of the DFT center. The center of DFT image represents frequency = 0 (u = 0 and v = 0) in the above images.

Frequency-Domain Filter Demonstration

In this section, the two-dimensional discrete-space sinusoids created in the previous section are added to an actual density image in the space domain. This process effectively creates spiral borehole noise on the FE image. **Figures 3b and 3c** show the simulated images, along with the original image in **Figure 3a**. The original image size is 64 × 256. The vertical length of 256 pixels represents 128ft in measured depth (MD). In other word, 2 pixels are equivalent to 1 foot (the depth interval = 0.5 ft).

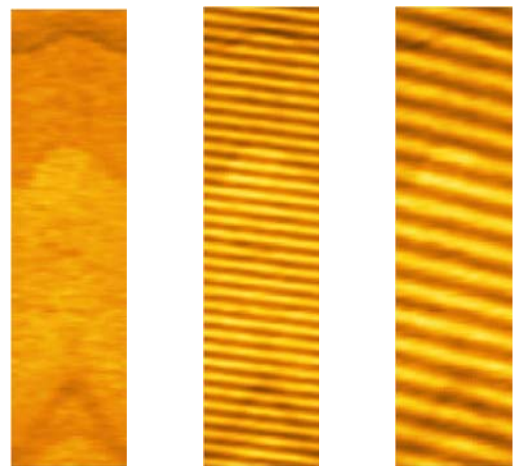

Figure 3a, 3b, and 3c: Original image and simulated images

As one can notice, it is very difficult to pick up formation features, such as dips and dip angles, in the noisy images in **Figures 3b and 3c**.

Now, we will apply the frequency-domain notch filter to the simulated FE images. **Figures 4a and 4b** show frequency masks (notch filter masks) in the DFT domain,

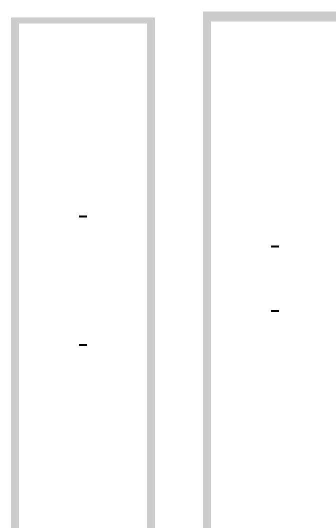

Figure 4a and 4b: Notch filter frequency masks

The filter mask has zero coefficients (black) at the oscillation frequency and ones (white) elsewhere. Gray frames are added to clarify the filter mask borders. Frequency = 0 (u = 0 and v = 0) is located at the center of the above masks.

The filter masks **Figures 4a and 4b** are applied to the simulated images from **Figures 3b and 3c**. The frequency-domain filtered images are shown below in **Figures 5b and 5c**, along with the original image in **Figure 5a**. The image size is 64 × 256. The vertical length of 256 pixels represents 128ft in measured depth (MD). In other word, 2 pixels are equivalent to 1 foot (the depth interval = 0.5 ft).

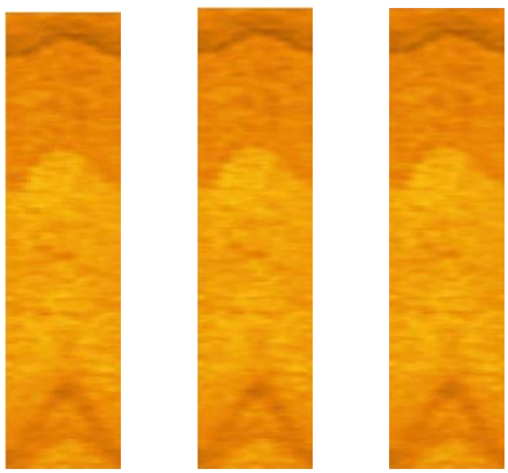

(5a) Original (5b) Restored **u = 32** (5c) Restored **u = 16**

Figure 5a, 5b, and 5c: Original image and restored images

As can be seen from the above figures, it is almost impossible to distinguish the difference among the original image and restored images (at least with the naked eye). Comparing the gray scale values (in the range 0-255) in these images, the maximum of 2 gray scale differences (out of 255) is noticed. However, most of the pixels have identical values. In the frequency-domain filtering process, it is observed that no side-effect (unwanted) noise is introduced in the restored images (**Figures 5b and 5c**).

More importantly, in the restored images, now it is possible to recognize the formation features and to apply dip-picking algorithms or any other feature-extraction algorithms.

Pure 2-D sinusoids are used exclusively for demonstration purposes; however, typical cyclic noise that appears on the actual FE images is often distorted and contains harmonic noise.

Software Implementation

A stand-alone ***Cyclic Noise Removal*** software has been developed to process various FE images. The algorithms introduced in this paper have been implemented in Visual Basic for Applications (VBA). The software is meant to be primarily used for research purposes. Currently this prototype software is not part of the surface software used at PathFinder®, A Schlumberger Company.

Additional Features

In order for the algorithm to work more effectively, the following three additional features have been implemented.

1) The software extracts the borehole oscillation information from caliper images and/or caliper logs, not from FE images.

2) One-dimensional DFT is applied to the caliper data to identify the oscillation frequencies, instead of using two-dimensional DFT.

3) The software searches for certain ranges of borehole oscillation periods/frequencies.

First, when the FE images are affected by borehole oscillation noise (even though various compensation algorithms try to minimize its negative effect), the noise is highly correlated to borehole shape measured in stand-off caliper images. Thus, to detect the oscillation noise in FE images more reliably, it is more effective to identify the oscillation noise observed in stand-off caliper images.

Secondly, to more efficiently identify the borehole oscillation frequencies, one-dimensional (1-D) DFT is applied to caliper data or azimuthal sectors of stand-off caliper image. The algorithm slices the caliper image vertically in the depth direction to take the DFT of the vertical slice. The 1-D DFT can be applied only to one azimuthal sector (one sector out of 64 or 32 sectors), several azimuthal sectors, or all azimuthal sectors (e.g. 8 sectors) if necessary. Oscillation frequencies can be extracted from caliper data measured with different tools, such as an RSS mechanical caliper[4,5].

Finally, most borehole oscillation problems are caused by the lower part of the BHA design, as pointed out in SPE115395. Namely, the majority of the oscillation frequency/period is related to the distance between the bit and the first touch point behind the bit[6,7]. Typically the first touch point behind the bit would be a near-bit stabilizer, a positive-displacement-motor (PDM) bend, or adjustable stabilizer/pads (in case of rotary steerable systems or RSS). Hence, the oscillation frequency range is predictable and, in some cases, the exact oscillation frequency could be calculated based on the lower part of the BHA spacing.

This software assumes no particular BHA and searches for the oscillation periods between 2ft/cycle and 10ft/cycle, which most of the conventional BHAs might produce (including a packed hole assembly, pendulum assembly, PDM, and RSS).

Software Input and Output

The software takes and outputs image files in LAS format. First, the stand-off caliper image file is read, and then either

RHOB or PE image file is processed based on borehole oscillation frequencies extracted from the caliper image file.

For quality control purposes, when the software scans the caliper image, it will generate an oscillation-noise-free image in LAS format. Hence, if the software reads all three files (caliper, ROHB and PE images), it generates three corresponding "processed" images in LAS format. These input files and processed files are later imported into our company's surface software or any other third-party software to generate image logs.

Graphical User Interface (GUI) design

Stand-alone cyclic noise removal software has been developed to examine the new noise removal algorithm. The software's GUI is very simple and intuitive, as shown in **Figure 6**.

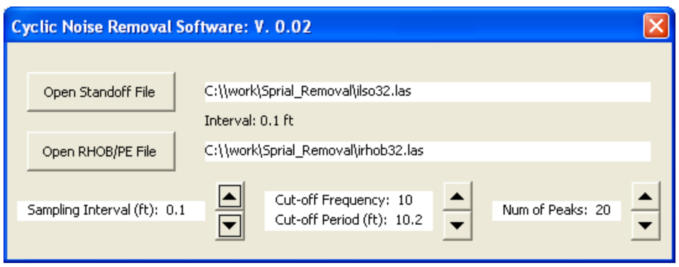

Figure 6: Cyclic Noise Removal Software GUI

On the left upper corner, there are two buttons: one is for selecting a stand-off caliper image file and the other for choosing either RHOB or PE image files (for the same depth interval).

On the bottom left corner, the user can select the sampling interval in ft specified in the LAS format. This value is typically between 0.1ft and 0.5ft.

On the bottom center, the user can enter a specific upper limit of the oscillation period in ft/cycle. The default value is set to 10ft/cycle, but if the lower part of the BHA spacing is known, the user can specify the upper limit. For example, the motor BHA has the near-bit stabilizer placed at 3ft from the bit and the motor bend located at 6ft from the bit, the user would select the upper limit to 7ft/cycle. This setting might increase the chance of accurate borehole oscillation noise removal from the FE images even though this user setting is optional.

Lastly, on the lower right corner, it shows the bandwidth of the notch (band-stop) filter around the center of the borehole oscillation frequencies.

This software does not have any image visualization features. The processed files in LAS format are later imported into our company's surface software or any other third-party software for log visualization and interpretation.

Well Examples

To assess the effectiveness of the new method, the algorithm is applied to field data from 3 different wells. The software was used to remove cyclic borehole noise primarily from bulk density images.

Well A

The LWD 4 ¾" density image tool was run at the GTI Gas Research Facility in Catoosa, Oklahoma. The well was drilled vertically to about 400ft and then gradually build angle to 93 degrees over 100ft towards the southeast. The well was first drilled down into a bed (~1225ft) and then drilled up out of the same bed (~1350ft).

The caliper and bulk density data are extracted from 1300ft to 1428ft (for the 128ft interval), and the Spiral Noise Removal Algorithm is applied to these images. **Figures 7a, 7b, 7c, and 7d** show the original caliper image (7a), processed caliper image (7b), original bulk density image (7c), and processed bulk density image (7d), respectively.

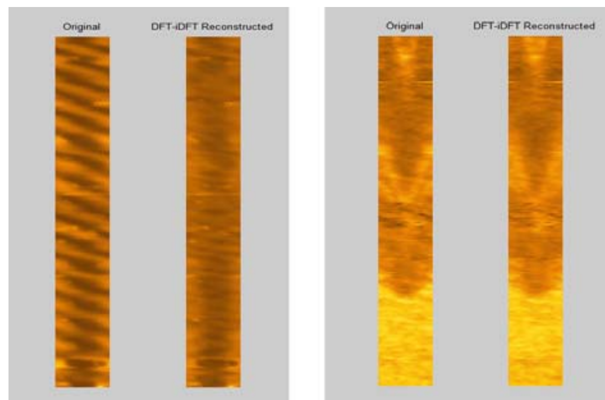

(7a) (7b) (7c) (7d)

Caliper images Bulk density images

Figure 7a, 7b, 7c and 7d: Original and processed images

As can be seen in **Figure 7b** (processed stand-off caliper image), the fundamental oscillation noise has been removed from the original stand-off caliper image in **Figure 7a**. Again, these stand-off caliper images are used for quality control purposes.

In **Figure 7c** (original bulk density image), borehole oscillation effect cannot be observed much because our company's stand-off compensation algorithm worked well for the small-amplitude spiral borehole. However, one can notice some improvements in the processed bulk density image in **Figure 7d**.

Well B

The horizontal section of the commercial well was drilled by adjusting up and down to stay in a carbonate reservoir. Density and PE images are used to optimize the pay interval.

Figures 8a, 8b, 8c, and 8d show the original acoustic standoff caliper image (8a), processed caliper image (8b), original bulk density image (8c), and processed bulk density image (8d), respectively.

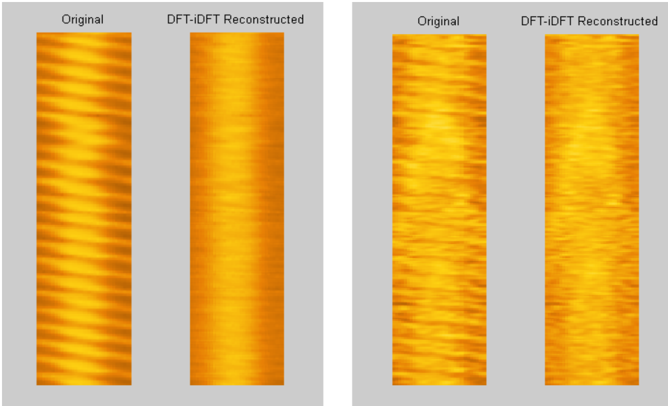

(8a) (8b) (8c) (8d)
Caliper images Bulk density images

Figure 8a, 8b, 8c and 8d: Original and processed images

As can be seen in **Figure 8b** (processed stand-off caliper image), the fundamental oscillation noise has been removed from the original standoff caliper image in **Figure 8a**. In the original bulk density image (**Figure 8c**), spiral borehole noise is observed; however, in the processed image (**Figure 8d**), oscillation noise is almost completely removed and small formation features can be identified more clearly. No PE images for the same interval are shown since they were not affected much from the oscillation noise.

Well C

Density and PE images are used in a similar commercial application as in Well B. In this 128ft interval, spiral direction was changed from right to left and from left back to right. This example has been chosen to see the response of the software algorithm to this particular spiral scenario.

Figures 9a, 9b, 9c, and 9d show the original acoustic caliper image (9a), processed caliper image (9b), original bulk density image (9c), and processed bulk density image (9d), respectively.

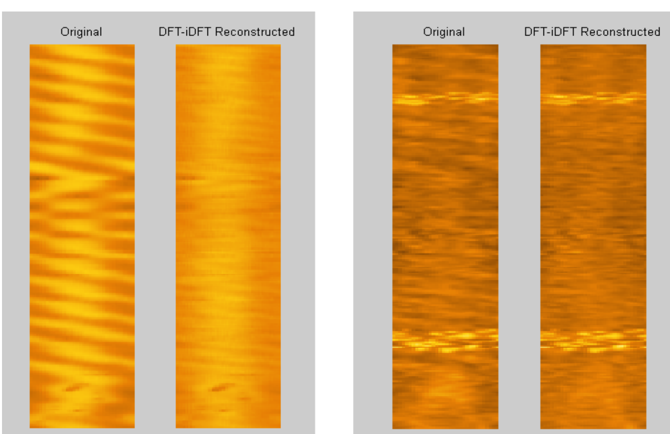

(9a) (9b) (9c) (9d)
Caliper images Bulk density images

Figure 9a, 9b, 9c and 9d: Original and processed images

As shown in **Figure 9b** (processed stand-off caliper image), the oscillation noise has been removed from the original standoff caliper image in **Figure 9a**. In the original bulk density image (**Figure 9c**), spiral borehole noise is slightly observed; however, in the processed image (**Figure 9d**), oscillation noise is greatly suppressed. No PE images for the same interval are shown since they were not affected much from the oscillation noise.

Conclusions

A new borehole-oscillation-noise removal algorithm from FE images has been demonstrated. The summary of our findings are listed below:

1) New two-dimensional frequency-domain filtering method removes and suppresses cyclic borehole noise from FE images.
2) In the examples shown in this paper, the noise removal algorithm does not remove formation features from the images.
3) Transformation process used in this new method does not add unwanted filter noise to the FE images.

Acknowledgments

We would like to thank PathFinder® for its willingness to provide the data obtained with IDNSC (Imaging Density Neutron Standoff Caliper) tools. We are grateful to PathFinder®, A Schlumberger Company, for permitting the publication of this work. Special thanks to Paul Boonen, Cornelis Huiszoon, Daniel Lai, Rick Lee and other Research Project members, for their valuable suggestions and comments.

Nomenclature

BHA	=	*Bottom Hole Assembly*
DFT	=	*Discrete Fourier Transform*
FE	=	*Formation Evaluation*
IDFT	=	*Inverse Discrete Fourier Transform*
LWD	=	*Logging While Drilling*
MWD	=	*Measurement While Drilling*
NB	=	*Near Bit*
PDM	=	*Positive Displacement Motor*
PE	=	*Photoelectric Effect*
ROP	=	*Drilling Rate Of Penetration*
RHOB	=	*Bulk Density* (ρ_b)
RPM	=	*Revolutions Per Minute*
RSS	=	*Rotary Steerable System*
WOB	=	*Weight On Bit*

References

1. Fitz, D. E., and Mills, A. A.: "Cyclic Noise in Open-hole and Cased-hole Logging Measurements: Its Impact and Remediation," SPE 84203 presented at the 2008 Annual Technical Conference and Exhibition, Denver, Colorado, 5-8 October 2003.
2. Nieto, J. A., Schmitt, D. P., and Keys, R. G.: "Removal of Borehole Induced Noise from Well Logs," paper III presented at

the 36th Annual SPWLA Symposium held in Oslo, Norway, 26-29 June 1995.
3. Nieto, J. A., Schmitt, D. P., and Keys, R. G., and Pann, K.: “Method for Removing Borehole Rugosity Noise from Well Log Data”, US Patent 5,579,247, Mobil, 26 November 1996.
4. Sugiura, J.: “Unique Imaging Techniques Optimize Push-The-Bit Borehole Quality”, AADE-09-NTCE-14-05 presented at the 2009 National Technical Conference and Exhibition, New Orleans, Louisiana, U.S.A., 4-7 April 2009.
5. Sugiura, J. and Jones, S.: “Closed-Loop Physical Caliper Measurements and Directional Drilling Method”, US Patent Application No. 20090090554, PathFinder Energy Services, 11 December 2008.
6. Sugiura, J., and Jones, S.: “The Use of the Industry’s First 3-D Mechanical Caliper Image While Drilling Leads to Optimized Rotary-Steerable Assemblies in Push- and Point-the-Bit Configurations”, SPE 115395 presented at the 2008 Annual Technical Conference and Exhibition, Denver, Colorado, 21-24 September 2008.
7. Sugiura, J.: “Novel Mechanical Caliper Image While Drilling and Borehole Image Analysis”, paper VV presented at the 50th Annual SPWLA Symposium held in Houston, Texas, 21-24 June 2009.